Surface Dipole Potential at the Interface between Water and Self-Assembled Monolayers of Phosphatidylserine and Phosphatidic Acid

Maria Rosa Moncelli, Lucia Becucci, Francesco Tadini Buoninsegni, and Rolando Guidelli
Department of Chemistry, Florence University, 50121 Florence, Italy

ABSTRACT The nature and magnitude of the surface dipole potential χ at a membrane/water interface still remain open to discussion. By combining measurements of differential capacity C and charge density σ at the interface between self-assembled monolayers of phosphatidylserine and phosphatidic acid supported by mercury and aqueous electrolytes of different concentration and pH, a sigmoidal dependence of χ upon σ is revealed, with the inflection at $\sigma = 0$. This behavior is strongly reminiscent of the surface dipole potential due to reorientation of adsorbed water molecules at electrified interfaces. The small increase in C with a decrease in the frequency of the AC signal below ~80 Hz, as observed with phospholipid monolayers with partially protonated polar groups, is explained either by a sluggish collective reorientation of some polar groups of the lipid or by a sluggish movement of protons across the polar head region.

INTRODUCTION

Even though the existence of an appreciable dipole potential difference between the interior of a membrane and the adjacent aqueous solution is universally accepted, the origin of this dipole potential remains obscure. Thus it may stem from the orientation of dipoles in 1) the water molecules adjacent to the membrane, 2) the polar headgroups, and/or 3) the ester linkages to the glycerol backbone (McLaughlin, 1977). The dipole potential χ is not a thermodynamically significant quantity, and hence cannot be measured directly. In principle, however, an insight into the origin of χ at membrane/water interfaces can be gained by measuring its changes with a change in the charge density σ_{lip} on the membrane surface. Incorporation of lipophilic ions into a membrane to change σ_{lip} is to be avoided, because these ions may easily alter the dipole potential by their very presence. A convenient procedure for altering the charge density of a phospholipid monolayer consists of changing the extent of protonation of its ionizable groups by varying the pH.

In recent years we have measured the charge density σ_{lip} of self-assembled monolayers of different phospholipids as a function of pH (Moncelli et al., 1994; Moncelli and Becucci, 1995), by using a biomimetic membrane that consists of a mercury electrode coated with a phospholipid monolayer (Miller, 1981; Nelson and Benton, 1986). This half-membrane provides an inherent mechanical stability and a resistance to high electric fields that are not shared by BLMs. Over the potential region of minimum capacity, which ranges from -0.15 to -0.75 V/SCE, the monolayer is impermeable to inorganic metal ions, whereas it becomes permeable outside this region. The differential capacity C of a lipid monolayer on mercury over this region is ~1.7–1.9 μF cm^{-2}, that is, twice the value for a BLM. The charge density σ_{lip} of a self-assembled monolayer of phosphatidylserine (PS) supported by mercury was found to vary from slightly negative to slightly positive values as the bulk pH of the bathing solution is varied from 7 to 4 (Moncelli et al., 1994). Analogously, the charge density σ_{lip} of a monolayer of phosphatidic acid (PA) passes from negative to positive values as the pH is varied from 4 to 1.5 (Moncelli and Becucci, 1995). PS and PA are therefore ideal candidates for measuring χ changes with varying pH.

In Moncelli at al. (1994) and Moncelli and Becucci (1995), the charge density σ_{lip} as a function of pH was determined by measuring the small changes in the overall differential capacity C of a lipid-coated mercury electrode after a change in the concentration of the electrolyte KCl from 5×10^{-3} to 0.1 M. These changes were considered to be due exclusively to a change in the differential capacity C_d of the diffuse layer, which can be regarded as being in series with the very low capacity, C_{lip}, of the monolayer; the reciprocal of the experimental capacity was therefore set equal to $1/C = 1/C_{lip} + 1/C_d$. The change in C_d after a given change in the electrolyte concentration c is expected to decrease rapidly with an increase in the absolute value of the overall charge σ experienced by the ions of the diffuse layer. Thus, if we plot values of the reciprocal, $1/C_d^{GC}$, of the diffuse-layer capacity calculated on the basis of the Gouy-Chapman (GC) theory at different electrolyte concentrations c and at constant charge σ against the corresponding values calculated at $\sigma = 0$, $1/C_{d,0}^{GC}$, we obtain roughly straight lines whose slope decreases progressively with an increase in $|\sigma|$, and ultimately vanishes for $|\sigma| \geq 4$ μC cm^{-2}. Because the capacity C_{lip} of the lipid monolayer is approximately independent of the electrolyte concentration, the slope, S_{exp}, of an experimental plot of $1/C$ against $1/C_{d,0}^{GC}$ for a given range of electrolyte concentrations was regarded as a measure of the slope of the plot of the reciprocal, $1/C_d$, of the experimental diffuse-layer capacity against $1/C_{d,0}^{GC}$. Slopes, S_{calc}, of

Received for publication 7 July 1997 and in final form 8 February 1998.
Address reprint requests to Dr. Rolando Guidelli, Department of Chemistry, Florence University, Via G. Capponi 9, 50121 Florence, Italy. Tel.: 39-55-2757540; Fax: 39-55-244102; E-mail: guidelli@cesit1.unifi.it.
© 1998 by the Biophysical Society
0006-3495/98/05/2388/10 $2.00

plots of the reciprocal $1/C_d^{GC}$ of the diffuse-layer capacity against $1/C_{d,0}^{GC}$ were therefore calculated on the basis of the GC theory at different pH values, for different sets of values of the protonation constants of the ionizable groups of the lipid. The resulting plots of S_{calc} versus pH were then compared with the experimental plot of S_{exp} versus pH for the lipid under study. Finally, the protonation constants of the lipid were ascribed the values providing the best fit between S_{exp} versus pH and S_{calc} versus pH plots. The overall charge density σ experienced by the diffuse-layer ions is the sum of the charge density on the lipid, σ_{lip}, plus the small charge density on the mercury surface, σ_M. Hence, to calculate S_{calc}, the charge density σ_M as a function of c and pH had also to be estimated. In doing so, we assumed that the surface dipole potential χ was independent of the solution composition, for simplicity.

In this work the simplifying assumption of a pH-independent surface dipole potential χ is abandoned. To draw conclusions about the pH dependence of χ, the charge density σ_M on PS- and PA-coated mercury electrodes was measured at different pH values. Moreover, the dependence of the differential capacity C upon the frequency ν was checked over the frequency range from 2 to 500 Hz. The results of these measurements suggest a contribution to χ from the reorientation of adsorbed water molecules; tentative explanations for the frequency dependence of C at frequencies less than 80 Hz will be provided.

EXPERIMENTAL

The water used was obtained from light mineral water by distilling it once, and by then distilling the water so obtained from alkaline permanganate, while constantly discarding the heads. Merck Suprapur® KCl was baked at 500°C before use to remove any organic impurities. Dioleoylphosphatidylcholine (PC) and dioleoyl PS were obtained from Lipid Products (South Nutfield, Surrey, England), and dioleoyl PA was obtained from Avanti Polar Lipids (Birmingham, AL). The desired pH values were realized with Merck Suprapur® HCl over the pH range from 2 to 5, with a 1×10^{-3} M $HPO_4^{2-}/H_2PO_4^-$ buffer over the pH range from 6.5 to 7.5, and with a 1×10^{-3} M H_3BO_3/NaOH buffer over the pH range from 8.5 to 9.8.

The home-made hanging mercury drop electrode (HMDE), the cell, and the procedure for the preparation of the self-assembled phospholipid monolayers are described elsewhere (Moncelli et al., 1994). Measurements of the differential capacity C at a constant frequency of 75 Hz were carried out with a Metrohm Polarecord E506 (Herisau, Switzerland). In view of the low capacity of the lipid-coated electrode (<2 μF cm^{-2}), C was directly measured by the quadrature component of the AC current, other than at the lowest salt concentrations; in the latter case, both quadrature and in-phase components of the AC current were measured, to correct for the cell resistance. The system was calibrated using a precision capacitor (Decade Capacitor type 1412-BC; General Radio, Concord, MA). All potentials were measured versus a saturated calomel electrode (SCE). The reproducibility of the differential capacity in passing from one mercury drop to another was better than 0.05 μF cm^{-2}. At any rate, each set of differential capacity measurements at variable KCl concentration and constant pH was carried out on the same lipid-coated mercury drop, so as to practically eliminate the effect of any slight irreproducibilities in the drop surface area or in the lipid transfer. This permitted us to estimate the changes in differential capacity after an increase in electrolyte concentration with an accuracy better than 0.02 μF cm^{-2}. The electrolyte concentration in the cell was progressively increased by adding a deaerated solution of the concentrated electrolyte from a microsyringe (Hamilton, Reno, NV). The plunger of the syringe was fastened tightly to the rod of a digital display micrometer screw with a 0.005-mm pitch (no. 297-101-01; Mitutoyo, Tokyo, Japan). The micrometer screw was held by a movable stand that permitted the syringe needle to be lowered into the solution during the addition and raised above the solution just after the addition. After each addition the solution was stirred mildly for ~30 s with a magnetic stirrer on the bottom of the cell. The stability of the differential capacity was tested by recording it over the whole potential region of minimum capacity two or three times consecutively, interposing a mild stirring between each measurement; whenever detectable differences between these recordings were observed, the whole series of measurements was discarded. Differential capacity measurements at different frequencies were carried out with a Stanford Research 850 lock-in amplifier. To check the stability of the lipid monolayer during measurements, the frequency of the AC signal was first varied progressively from 2 to 500 Hz, and then in the opposite direction on the same lipid-coated mercury drop. Measurements were discarded whenever the difference in the capacity values at the same frequency in the two opposite runs was found to be greater than 1%.

The surface charge density σ_M at the HMDE coated with a self-assembled phospholipid monolayer was measured by a technique described elsewhere (Becucci et al., 1996). Briefly, σ_M was obtained by analogical integration of the capacitive current that flows at constant applied potential as a consequence of a slight contraction of the mercury drop. The contraction must be carried out while keeping the neck of the lipid-coated mercury drop in contact with the lipid film spread on the surface of the electrolytic solution. This procedure ensures that the monolayer maintains its properties, including its thickness, as the drop is expanded or compressed. The capacitive charge flowing during a change ΔA in the drop area, once divided by ΔA, yields directly the charge density σ_M on the metal.

RESULTS

Protonation

Fig. 1 shows plots of S_{exp} versus pH for PS- and PA-coated mercury electrodes. Both plots show a maximum. In the

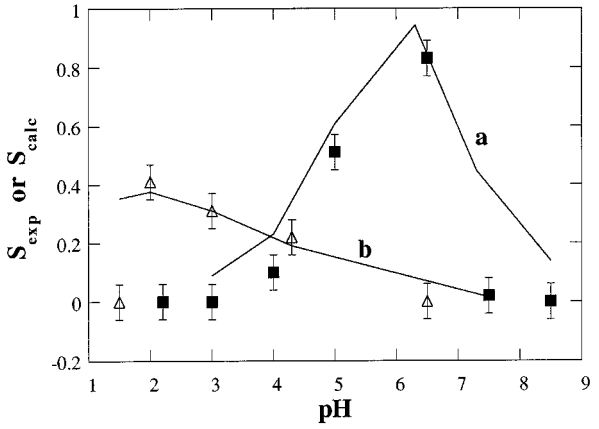

FIGURE 1 Values of S_{exp} versus pH for PS (■) and PA (△) self-assembled monolayers supported by mercury. The solid curves are S_{calc} versus pH plots calculated as described in the text for PS, with $K_1 = 5 \times 10^6\ M^{-1}$, $K_2 = 1 \times 10^5\ M^{-1}$, and $\gamma/\epsilon_\gamma = 0.1 \times 10^{-8}$ cm (*a*), and for PA with $K_1 = 1 \times 10^8\ M^{-1}$, $K_2 = 1 \times 10^5\ M^{-1}$, $K_3 = 50\ M^{-1}$, and $\gamma/\epsilon_\gamma = 0.2 \times 10^{-8}$ cm (*b*).

case of PS, S_{exp} is practically zero at pH 7.5, which implies that at this pH value the polar head is negatively charged. The S_{exp} value approaching unity in the proximity of pH 6 indicates that the polar head of PS is practically neutral at this pH. This implies that one of the two anionic groups, either the phosphate or the carboxyl group, is almost completely protonated; in this way, the negative charge borne by the other anionic group is practically neutralized by the positive charge of the amino group, which is completely protonated over the whole pH range investigated. As the pH is decreased further from 6 to 3, the S_{exp} value decreases again, attaining the zero value: this implies that the polar head is now positively charged, and hence that even the further anionic group starts to be appreciably protonated. To justify the very weak acidity of at least one of the two anionic groups, we must necessarily assume that it is buried somewhere inside the polar head region of PS (Moncelli at al., 1994). In such a position an anionic group has a much lower acidity than in bulk water, because the negative average potential difference between the position of the anion and the aqueous solution attracts protons electrostatically; moreover, the reaction of the monoanion with a proton annihilates the charges of both reactants, and hence is strongly favored by the low dielectric constant of the polar head region. Of the two anionic groups, the one that is likely to be more deeply buried in the polar head region is the phosphate group, because of its closer vicinity to the hydrocarbon tails. As concerns the PA film, the $-PO_4^{2-}$ group is monoprotonated over the whole pH range investigated. The fact that S_{exp} becomes different from zero at pH less than 5 denotes a further protonation of the phosphate group and a resulting tendency of the polar heads to become uncharged. However, the rapid decay of S_{exp} in passing from pH 2 to pH 1.5 can only be explained by a tendency of the polar heads to become positively charged at these low pH values. A possible explanation is a labile binding of a proton to the >C═O group of one of the ester groups of the lipid (Moncelli and Becucci, 1995).

Charge measurements

Fig. 2 shows the charge density σ_M on PS- and PA-coated mercury in 0.1 M KCl at a constant applied potential of −0.5 V as a function of pH. In the case of the PS film, σ_M attains a maximum value in the proximity of pH 5, where the PS polar head is almost uncharged, and then decreases again with a further increase in pH. A decrease in σ_M with an increase in pH is also observed with the PA film. This behavior contradicts our original assumption of a pH-independent dipole potential χ (Moncelli et al., 1994; Moncelli and Becucci, 1995). If this assumption were correct, then the charge density σ_M at constant applied potential would shift gradually in the positive direction with an increase in pH, to compensate for the negative shift in the surface potential ψ_d after the progressive deprotonation of the ionizable groups. The behavior of the σ_M versus pH plots in Fig. 2 denotes an appreciable change in χ with a change in pH.

Frequency dispersion

The frequency dependence of the differential capacity C of self-assembled monolayers of PS, PA, and PC in contact with aqueous solutions of 0.1 M KCl of different pH values is shown in Figs. 3 and 4 over the frequency range from 2 to 500 Hz at a bias potential of −0.5 V. With all systems investigated, C is independent of the frequency ν for $\nu \geq 80$ Hz. However, as the frequency is decreased below this value, the PS and PA films start to show a small but progressive increase in C that is still observed at 2 Hz. This frequency dispersion is observed at all pH values investigated, but is more pronounced at the lower pH values. The behavior of PC differs from that of PS and PA in that no frequency dispersion is observed at pH greater than 4; only

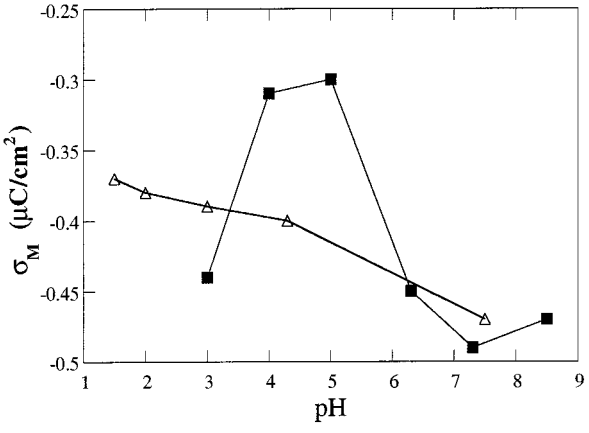

FIGURE 2 Values of σ_M versus pH for PS (■) and PA (△) self-assembled monolayers supported by mercury in 0.1 M KCl at −0.5 V/SCE.

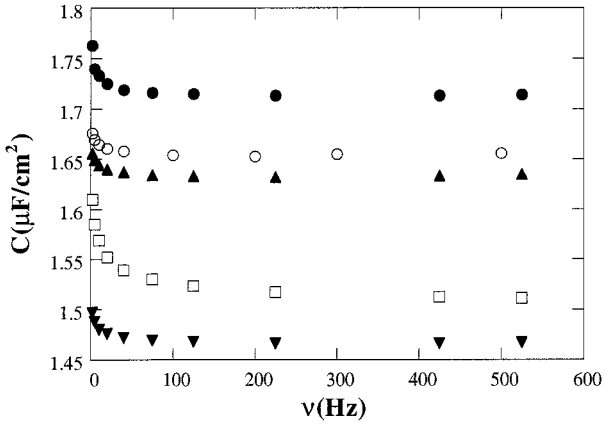

FIGURE 3 Plots of C versus ν for a PS self-assembled monolayer at −0.5 V/SCE in 0.1 M KCl-buffered solutions of pH 4.3 (▼), 3.2 (□), 5.3 (▲), 7.3 (○), and 6.3 (●).

at lower pH values does the differential capacity increase slightly with a decrease in frequency below 80 Hz.

DISCUSSION

Frequency dependence of the differential capacity

In view of the complexity of the structure of the self-assembled lipid monolayer, the frequency dispersion in Figs. 3 and 4 cannot be ascribed unambiguously to a single phenomenon. Thus, in principle, any movement of charged species or reorientation of dipoles within the lipid film that is in a condition of following the small (10 mV peak-to-peak) AC signal will oppose the corresponding external alternating field with a resulting increase in differential capacity; only when a sufficiently high increase in frequency causes this charge movement and/or dipole reorientation to lag behind the AC signal will the differential capacity attain a constant minimum value. A sluggish change in the tilt of the hydrocarbon tails of the lipid after the AC signal, with a resulting change in the thickness of the film and in its differential capacity, seems to be excluded. In fact, it would be expected not only with PS and PA, but also with PC, because all of these lipids have the same dioleoyl hydrocarbon tails. Moreover, it cannot explain the passage from a frequency independence of C to a frequency dispersion with a decrease in pH, as observed with PC films (see Fig. 4). The frequency dispersion in Figs. 3 and 4 can be tentatively explained 1) by a sluggish collective reorientation of some polar groups of the lipids after the AC signal, or 2) by a sluggish movement of protons from partially protonated ionizable groups buried inside the polar head region to the bathing solution and vice versa.

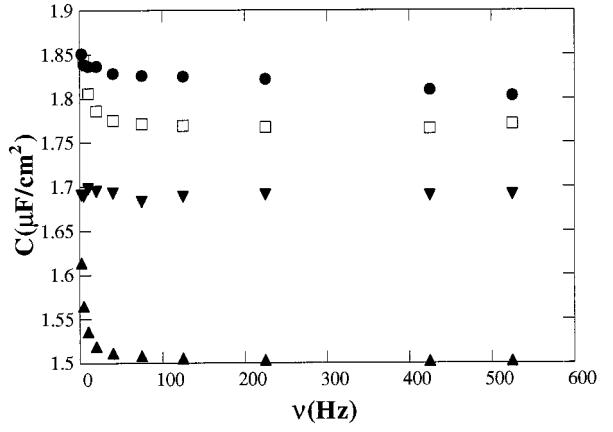

FIGURE 4 Plots of C versus ν for a PC self-assembled monolayer at −0.5 V/SCE in 0.1 M KCl-buffered solutions of pH 1.8 (●) and 7.5 (▼), and for a PA self-assembled monolayer at −0.5 V/SCE in 0.1 M KCl-buffered solutions of pH 1.5 (▲) and 7.2 (□).

In the first case the change in orientation of the polar heads of the lipid after the small AC signal must also be very small. Thus, e.g., if the dipole moment μ of the dipole consisting of the charged carboxyl group and of the charged ammonium group in a PS molecule is estimated at 6 D, the change in χ involved in its passage from an orientation parallel to the monolayer to a vertical orientation amounts to $4\pi N N_A \mu/\epsilon_\gamma$, where $N \approx 2 \times 10^{-10}$ mol cm^{-2} is the density of PS in the monolayer, N_A is Avogadro's number, and ϵ_γ is the dielectric constant of the polar head region. If we set $\epsilon_\gamma = 30$, the change in χ is equal to 0.09 V and involves a charge flow of about (2 μF cm^{-2}) × 0.09 V = 0.18 μC cm^{-2}; if the AC signal of 10 mV peak-to-peak were to produce such a drastic reorientation of the above dipole moment, it would give rise to an increase in differential capacity as high as 18 μF cm^{-2}. A slight change in the orientation of the polar heads of a PS monolayer supported on Hg can be tentatively justified by considering that the acidity of the phosphate group in this monolayer is much lower than that normally reported in the literature for PS vesicles (Tsui et al., 1986), dispersions (MacDonald et al., 1976), monolayers (Ohki and Kurland, 1981), and BLMs (Matinyan et al., 1985), where the electric field acting on the hydrocarbon tails and the parameters related to intermolecular spacing and state of compression may be somewhat different. In Moncelli at al. (1994), this difference in behavior was explained by assuming that PS self-assembled monolayers may assume at least two different conformations of the polar head, with similar Gibbs energies but quite different acidities of the ionizable groups. Thus a conformation of the PS polar heads with two negative and one positive charge on the same plane parallel to the lipid layer is not as electrostatically favored as the conformation assumed by zwitterionic lipids such as PC: a conformation with the phosphate group deep inside the polar head region and a C-N dipole roughly parallel to the lipid plane and in direct contact with the aqueous phase may well have a comparable Gibbs energy. This interpretation of the apparently anomalous behavior of PS self-assembled monolayers is supported by the observation that in the presence of adsorbed tetraphenylphosphonium cations, these monolayers behave as though they were actually negatively charged

(Moncelli et al., 1995); this behavior was explained by a conformational change in the PS polar heads induced by the tetraphenylammonium cations, leading to a deprotonation of the phosphate groups. It is therefore possible that at frequencies less than 80 Hz, the applied AC field may start to be accompanied by a modest fluctuation in the conformation of the PS polar heads.

An alternative explanation for the increase in differential capacity with a decrease in frequency below ~80 Hz consists of assuming a progressive increase in the ability of the protons to move to and fro across the polar head region after the AC signal, and hence to oppose the applied AC field. This implies a slow equilibration of the protons between the polar head region of the lipid film and the bathing solution. This interpretation contrasts with kinetic analyses of time-resolved proton-phospholipid interactions in micelles and liposomes (Nachliel and Gutman, 1988; for a review see Gutman and Nachliel, 1990), according to which the rate of proton binding to the phospholipid lies in the microsecond and submicrosecond time scale. Gutman's conclusions tend to support the "delocalized chemiosmotic theory" (Kasianowicz et al., 1987; Polle and Junge, 1989), according to which the proton movement from proton pumps to proton sinks in photosynthesis and respiration takes place in the aqueous bulk phase because of a very rapid equilibration of the protons between the lipid and the adjacent bathing solution. However, in several laboratories, evidence has also been gathered in favor of a "localized theory," according to which protons move exclusively along the membrane surface; the latter evidence relies on measurements with both biomimetic membranes (Kell, 1979; Prats et al., 1985, 1986; Teissié et al., 1985; Morgan et al., 1988; Antonenko et al., 1993) and fragments of biomembranes. Thus Heberle et al. (1994) showed that a pH sensor positioned at the surface of a purple membrane, at an average distance of 240 nm from the proton ejecting bacteriorhodopsin, detects the liberated protons eight times faster than a pH probe in the bulk aqueous phase at an average distance of only 17 nm. According to these authors, the proton's lateral motion along the membrane surface is faster than in the adjacent bulk water phase, not because of a higher diffusion coefficient of protons, but rather because of a surprisingly low rate of proton transfer from the membrane surface to the water phase, lying in the millisecond time scale; protons should therefore move within an extended Coulomb cage formed by the lipid headgroups and the proteinous amino acids. An interpretation of the frequency dispersion in Figs. 3 and 4 in terms of a slow equilibration of protons between the polar head region of the lipid monolayer and the bulk aqueous phase would therefore provide a further piece of evidence in favor of the delocalized theory.

Under the assumption that the frequency dispersion is due to sluggish protonation equilibria, the experimental S_{exp} versus pH plots in Fig. 1 refer to a situation in which these protonation equilibria do not follow the AC signal, because they were obtained at a frequency of 75 Hz, which practically marks the upper boundary of the region of frequency dispersion, as appears from Figs. 3 and 4. The two-capacitor model adopted in the previous work carried out in this laboratory (Moncelli et al., 1994) does not account for this situation, because it locates all ionizable groups in direct contact with the aqueous phase; moreover, the capacity C includes a finite contribution due to the rate of change, $d\sigma_{lip}/d\sigma_M$, of the overall charge density σ_{lip} of the polar heads of the lipid with a change in σ_M. If σ_M is shifted in the positive direction, protons are repelled electrostatically from the aqueous phase in the immediate vicinity of the lipid film, increasing the local pH there; this causes an instantaneous partial deprotonation of the ionizable groups of the lipid and a decrease in σ_{lip}. In practice, a protonation-deprotonation step with a relaxation time much shorter than the period, ν^{-1}, of the AC signal causes the term $d\sigma_{lip}/d\sigma_M$ to be negative. On the other hand, if its relaxation time is much longer than ν^{-1}, the term $d\sigma_{lip}/d\sigma_M$ tends to vanish, causing a decrease in the differential capacity C.

A model of the mercury/phospholipid/water interphase

In what follows we will adopt a model of three capacitors in series, schematically depicted in Fig. 5, to account for a possible slow equilibration of protons. The model will only consider the two extreme situations in which the protonation equilibria involving the ionizable groups buried well inside the polar head region either follow the AC signal perfectly or else do not follow it at all, and hence are blocked at the bias potential. This model will serve to show that the experimental frequency dispersion can be justified by assuming that certain protonation equilibria are blocked at frequencies greater than 80 Hz, and hence that their contribution to σ_{lip} does not follow the fluctuations of σ_M produced by the AC signal. Fig. 5 shows a model of a lipid monolayer deposited on mercury, consisting of a hydrocarbon tail region of dielectric constant ϵ_β enclosed between the electrode surface plane $x = 0$ and the plane $x = \beta$, and of a polar head region of dielectric constant ϵ_γ enclosed between $x = \beta$ and the lipid/solution boundary $x = d \equiv (\beta$

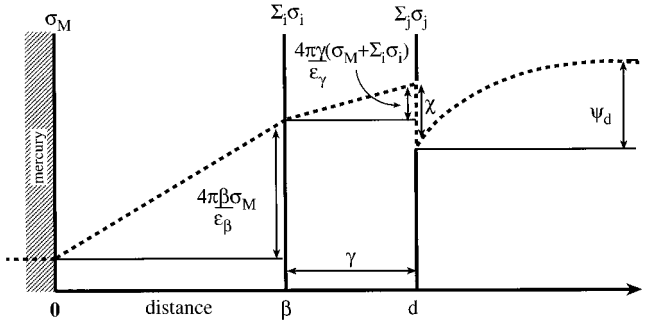

FIGURE 5 Schematic picture of the model for a lipid monolayer deposited on mercury. The dashed curve schematically represents the profile of the average potential against the distance from the mercury surface. The diffuse-layer thickness has been compressed with respect to the monolayer thickness, for ease of representation.

$+ \gamma$) (Moncelli et al., 1995). For simplicity, the ionizable groups of the lipid are considered to be located either at the boundary $x = \beta$ between these two regions, or else at $x = d$, that is, in direct contact with the aqueous phase. The groups at $x = d$ experience a hydrogen ion concentration satisfying the Boltzmann distribution law, i.e., $c_{H+} \exp(-F\psi_d/RT)$, where c_{H+} is the bulk hydrogen ion concentration and ψ_d is the "average" electric potential at $x = d$, i.e., the surface potential. The hydrogen ion concentration at $x = \beta$ is also assumed to satisfy a Boltzmann distribution law, $c_{H+} \exp(-F\phi_\beta/RT)$; in this case, however, the electric potential ϕ_β at $x = \beta$ is considered to have a local character, and hence to experience discreteness-of-charge effects. These effects are considered in the framework of the "cutoff disk model," according to which an adsorbed ion is surrounded by a circular charge-free region (the exclusion disk) that is imaged infinite times in the $x = 0$ and $x = d$ planes (Levine et al., 1962, 1965). The expected values for the parameters of a typical lipid monolayer are 10–20 Å for β, 4–10 Å for γ, ~2 for ϵ_β, and 8–50 for ϵ_γ (Flewelling and Hubbell, 1986). Moreover, the cross-sectional area of a lipid molecule is close to 60 Å^2; hence, if each polar head contains only one ionizable group at $x = \beta$, the "steric hard-core radius" between two neighboring ionizable groups is on the order of 8–9 Å. The exclusion disk radius, ρ, cannot be smaller than this steric hard-core radius. With such a large value for ρ, Levine's expression for the local potential ϕ_β, as measured with respect to the bulk solution, is satisfactorily approximated by its limiting form for $\rho \to \infty$ (Levine et al., 1972; Moncelli et al., 1995):

$$\phi_\beta = \frac{\gamma/\epsilon_\gamma}{\beta/\epsilon_\beta + \gamma/\epsilon_\gamma}(\psi_0 - \chi - \psi_d) + \psi_d \qquad (1)$$

In fact, when ρ is comparable to the distance 2γ between the discrete charges at $x = \beta$ and their nearest-neighboring images, the screening effect of these images becomes so large as to cause the limiting behavior for $\rho \to \infty$ to be closely approached.

For the sake of generality, let us denote the set of charge densities due to the ionizable groups at $x = \beta$ by $\{\sigma_i\}$, and that due to the ionizable groups at $x = d$ by $\{\sigma_j\}$, where the subscripts i and j refer to the different groups. The average potential difference ψ_0 across the whole interface will then be given by

$$\psi_0 = 4\pi\frac{\beta}{\epsilon_\beta}\sigma_M + 4\pi\frac{\gamma}{\epsilon_\gamma}(\sigma_M + \Sigma_i\sigma_i) + \chi + \psi_d \qquad (2)$$

Here the first term is the average potential difference across the hydrocarbon tails, whereas the second is that across the polar head region; according to the GC theory, the potential difference ψ_d across the diffuse layer is a function of c, σ_M, and the overall charge density of the lipid, $\sigma_{lip} = \Sigma_i\sigma_i + \Sigma_j\sigma_j$. If all protonation equilibria are perfectly mobile, differentiation of Eq. 2 with respect to σ_M yields the following expression for the reciprocal of the differential capacity C:

$$\frac{1}{C} = \frac{d\psi_0}{d\sigma_M} = 4\pi\left(\frac{\beta}{\epsilon_\beta} + \frac{\gamma}{\epsilon_\gamma}\right) + 4\pi\frac{\gamma}{\epsilon_\gamma}\frac{d(\Sigma_i\sigma_i)}{d\sigma_M} + \frac{d\psi_d}{d(\sigma_M + \sigma_{lip})} \cdot \left(1 + \frac{d\sigma_{lip}}{d\sigma_M}\right) \qquad (3)$$

where $d\chi/d\sigma_M$ is now regarded as negligibly small. At frequencies high enough to block the movement of protons across the polar head region ($\beta < x < d$), the derivatives $d\sigma_i/d\sigma_M$ vanish, and Eq. 3 becomes

$$\frac{1}{C} = 4\pi\left(\frac{\beta}{\epsilon_\beta} + \frac{\gamma}{\epsilon_\gamma}\right) + \frac{d\psi_d}{d(\sigma_M + \sigma_{lip})}\left[1 + \frac{d(\Sigma_j\sigma_j)}{d\sigma_M}\right] \qquad (4)$$

For an uncharged lipid, the differential capacity is approximately given by $[4\pi(\beta/\epsilon_\beta + \gamma/\epsilon_\gamma)]^{-1}$, once we neglect the small contribution from the diffuse layer. This quantity can be accurately estimated at 1.7 μF cm^{-2}, which corresponds to the differential capacity of an uncharged PC monolayer. Because all of the features of the lipid monolayer, apart from the protonation constants, depend exclusively upon the β/ϵ_β and γ/ϵ_γ ratios, only one of these two parameters is adjustable, whereas the other is obtained from the relation $[4\pi(\beta/\epsilon_\beta + \gamma/\epsilon_\gamma)]^{-1} \approx 1.7$ μF cm^{-2}. In particular, if we ascribe to β and ϵ_β the reasonable values 10 Å and 2, the γ/ϵ_γ ratio turns out to be equal to 0.21×10^{-8} cm in electrostatic CGS units. A treatment of the model is outlined in the Appendix.

The solid curve *a* in Fig. 1 shows the S_{calc} versus pH plot for PS in best agreement with the corresponding S_{exp} versus pH plot, as calculated on the basis of the model by assuming that the phosphate and carboxyl groups are located at $x = \beta$, with $\gamma/\epsilon_\gamma = 0.1 \times 10^{-8}$ cm, and by setting the protonation constants of these two groups equal to $K_1 = 5 \times 10^6$ M^{-1} and $K_2 = 1 \times 10^5$ M^{-1}. The plot was calculated by regarding the protonation equilibria of these groups as blocked at the bias potential $E = -0.5$ V; in other words, the protons of the phosphate and carboxyl groups were considered to be unable to follow the 75-Hz AC signal. Incidentally, over the pH range investigated, the amino group of PS is fully protonated and therefore does not contribute to the movement of protons after the AC signal. Curve a in Fig. 6 shows a plot of ΔC versus pH, where ΔC is the difference between the differential capacity values estimated for the two extreme situations in which the protonation equilibria follow the AC signal perfectly or else are blocked at the bias potential; naturally, when we assumed that all protonation equilibria are perfectly mobile through the use of Eq. 4, the differential capacity was calculated by using a different set of protonation constants, i.e., the set that provides the best agreement with experiment under these assumptions. In practice, ΔC measures the maximum frequency dispersion resulting from the lack of proton equilibration. As expected, the maximum frequency dispersion is attained in the proximity of the pH values corresponding to the log K values of the ionizable groups buried in the polar

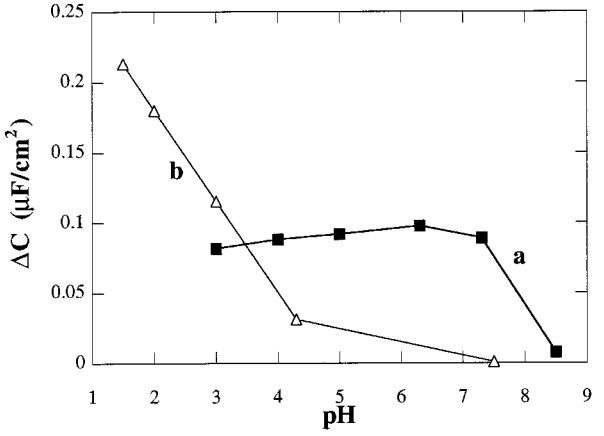

FIGURE 6 Plots of ΔC versus pH for PS (■) and PA (△) self-assembled monolayers supported by mercury, calculated as described in the text.

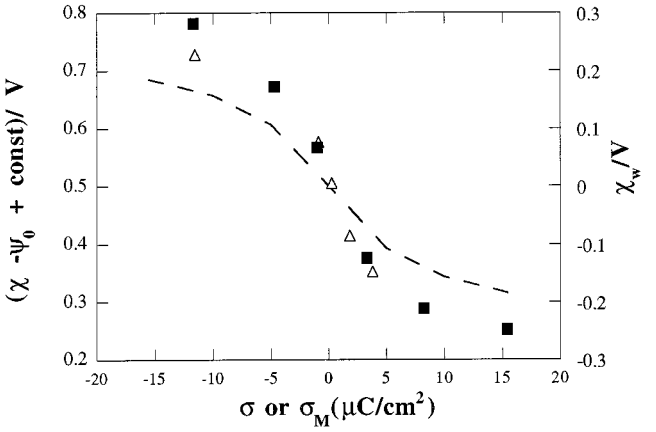

FIGURE 7 Plots of (χ-ψ_0 + const) versus σ for PS (■) and PA (△) self-assembled monolayers at −0.5 V/SCE in buffered solutions of 0.1 M KCl, calculated as described in the text. The dashed curve is a χ_w versus σ_M plot calculated by Damaskin and Frumkin (1974) for a metal/water interphase.

head region, namely at those pH values at which the concentrations of the protonated and deprotonated forms of these groups are comparable. The model predicts the correct order of magnitude of the experimental frequency dispersion shown in Figs. 3 and 4.

The solid curve b in Fig. 1 shows the S_{calc} versus pH plot for the PA film in best agreement with the corresponding S_{exp} versus pH plot, as calculated by assuming that the proton loosely bound to the >C═O group of one of the ester groups of the lipid is located at $x = \beta$ and does not follow the 75-Hz AC signal. Conversely, the phosphate group is located at $x = d$ and follows the AC signal. The protonation constant K_3 of the group buried inside the polar head region that provides the best agreement with experiment equals 50 M^{-1}, whereas those for the two consecutive protonation equilibria of the phosphate group are equal to $K_1 = 1 \times 10^8$ M^{-1} and $K_2 = 1 \times 10^5$ M^{-1}. Curve b in Fig. 6 shows the plot of ΔC versus pH for the PA film, where ΔC is the increment in the calculated value of C if the protonation equilibrium of the group located at $x = \beta$ were perfectly mobile.

The surface dipole potential

The plot of χ-ψ_0 = (χ + const.) versus σ resulting from the use of the model in Fig. 5 is shown in Fig. 7; it exhibits a sigmoidal shape, with the maximum slope lying in the proximity of $\sigma = 0$. This plot is reminiscent of the surface dipole potential χ_w due to the water molecules adsorbed at a metal/water interface as a function of the charge density σ_M on the metal. For comparison, the dashed curve in Fig. 7 is a plot of χ_w versus σ_M, as calculated by Damaskin and Frumkin (1974) on the basis of a simple model of the metal/water interface. Moreover, the magnitude of the maximum change of χ in the (χ + const.) versus σ plots of Fig. 7 is comparable with that estimated by Trasatti (1975) (~300 mV) for the interface between the hydrophilic liquid gallium and water on the basis of several pieces of experimental evidence combined with a minimum of modelistic assumptions. This strongly suggests that the change in χ with varying charge density of the PS and PA monolayers is mainly to be ascribed to the reorientation of the water molecules in contact with the polar heads; this conclusion is supported by the consideration that the only dipoles that experience the whole charge σ_{lip} on the lipid must lie outside the lipid film. Similar conclusions as to the molecular origin of the surface dipole potential in lipid films were drawn by Gawrisch et al. (1992) and by Zheng and Vanderkooi (1992). The surface dipole potential associated with the ester linkages to the glycerol backbone, which has been regarded as responsible for the higher permeability in lipid bilayers of lipophilic anions with respect to cations (McLaughlin, 1977; Honig et al., 1986), is apparently unaffected by a change in σ_{lip}. Naturally, some caution must be used in transferring these conclusions to biological membranes, which incorporate integral proteins protruding for 10 Å or so outside the lipid leaflet. Nonetheless, over the patches of the lipid leaflet free from proteins, the contribution of water reorientation to the surface dipole potential is expected to be appreciable.

It should be noted that a plot of (χ + const.) versus σ with a sigmoidal shape and the maximum slope lying in the proximity of $\sigma = 0$ are also obtained by using the crude two-capacitor model adopted in Moncelli et al. (1994), in which the ionizable groups are assumed to be in direct contact with the aqueous phase and their protonation equilibria are perfectly mobile; naturally, with this model the protonation constants providing the best fit between the S_{calc} versus pH plots and the corresponding S_{exp} versus pH plots of Fig. 1 assume different values. Hence the sigmoidal dependence of the surface dipole potential upon the charge is not subordinated to the assumption of a lack of proton equilibration.

CONCLUSIONS

A completely unambiguous explanation cannot be found for the slight increase in differential capacity as the frequency of the AC signal is decreased below 80 Hz (see Figs. 3 and 4), although it may be justified either by a sluggish collective reorientation of some polar groups of the lipids after the AC signal, or else by a sluggish movement of protons from partially protonated ionizable groups buried inside the polar head region to the bathing solution, and vice versa. The lack of frequency dispersion shown by PC monolayers over a broad pH range from 4 to 9 (see Fig. 4) can be justified equally well on the basis of any of the above two tentative arguments. Thus, over this pH range, the PC film is uncharged and does not contain partially protonated ionizable groups such as to justify a movement of protons. On the other hand, over this pH range the conformation of the PC polar heads with the P-N dipoles aligned head to tail in the directions parallel to the monolayer is the most energetically favored arrangement from an electrostatic viewpoint, such as to resist changes after the AC signal. As the pH is decreased below 3, the incipient protonation of the phosphate groups begins to convert a number of P-N zwitterions into -N$(CH_3)_3^+$ cations, thus undermining the network of parallel P-N dipoles. As a result, the residual P-N dipoles will tend to assume a tilted orientation that, by creating a favorable potential difference across the polar head region, will cause the protons to be attracted toward the innermost portion of this region and to protonate the phosphate groups there (Moncelli et al., 1994). Hence, at pH less than 3, the AC signal may cause either a very small fluctuation in the tilt of the P-N dipoles or a movement of protons from the partially protonated phosphate groups to the aqueous phase, and vice versa: either of these two movements may be sluggish enough to lag behind the AC signal at frequencies greater than 80 Hz, justifying the slight frequency dispersion shown by PC at pH 1.8 (see Fig. 4).

APPENDIX

The sum of the charge density σ_M on the metal surface and that of the lipid, $\sigma_{lip} = \Sigma_i\sigma_i + \Sigma_j\sigma_j$, is equal and opposite that of the diffuse-layer ions. According to the GC theory, this statement is expressed by the following implicit function:

$$\sigma_M + \sum_i \sigma_i + \sum_j \sigma_j - A(1/y - y) \equiv g = 0 \quad \text{(A1)}$$

with

$$A \equiv \sqrt{\frac{RT\epsilon(c + c_{H^+})}{2\pi}}; \qquad y \equiv \exp\left(-\frac{F\psi_d}{2RT}\right) \quad \text{(A2)}$$

Here c is the bulk concentration of the 1,1-valent electrolyte used to vary the ionic strength, c_{H+} is the bulk concentration of hydrogen ions, and $\epsilon = 78$ is the dielectric constant of the solvent.

Let us assume that the protons bind to the ionizable groups of the lipid according to a Langmuir isotherm. Moreover, let us denote by $\sigma_{max,i}$ ($\sigma_{max,j}$) the maximum charge density attainable by the ith (jth) ionizable group. The charge density σ_i of the ith ionizable group located at $x = \beta$ will then be given by

$$\sigma_i = \frac{\sigma_{max,i}}{1 + K_i[H^+]_\beta} \quad \text{or} \quad \sigma_i = \frac{\sigma_{max,i}K_i[H^+]_\beta}{1 + K_i[H^+]_\beta} \quad \text{(A3)}$$

depending on whether $\sigma_{max,\,i}$ is negative or positive. Here K_i is the protonation constant of the ith group, and $[H^+]_\beta$ is the proton concentration at $x = \beta$ as affected by the local potential ϕ_β. In view of the expression of Eq. 1 for ϕ_β, we have

$$[H^+]_\beta = c_{H^+}\exp\left(-\frac{F\phi_\beta}{RT}\right) = c_{H^+}\exp\left(-\frac{F}{RT}\frac{\gamma'}{\gamma' + \beta'}\psi'_0\right)y^{2\beta'/(\gamma'+\beta')} \quad \text{(A4)}$$

where we have set

$$\psi'_0 \equiv \psi_0 - \chi; \qquad \beta' \equiv \beta/\epsilon_\beta; \qquad \gamma' \equiv \gamma/\epsilon_\gamma \quad \text{(A5)}$$

to simplify notations. By analogy with Eq. A3, the charge density σ_j of the jth ionizable group at the boundary $x = d$ of the lipid film with the aqueous phase is given by

$$\sigma_j = \frac{\sigma_{max,j}}{1 + K_j c_{H^+}y^2} \quad \text{or} \quad \sigma_j = \frac{\sigma_{max,j}K_j c_{H^+}y^2}{1 + K_j c_{H^+}y^2} \quad \text{(A6)}$$

depending on whether $\sigma_{max,j}$ is negative or positive; K_j is the protonation constant of the jth group, and $c_{H+}\exp(-F\psi_d/RT) = c_{H+}y^2$ is the hydrogen ion concentration at $x = d$. Strictly speaking, Eqs. A3 and A6 do not apply to the consecutive protonations of a multiply charged ionizable group, such as the -PO_4^{2-} group of PA. However, it can be readily shown that the above equations are still valid, provided that the first protonation constant is both much greater than the second and much greater than $1/c_{H+}$ over the pH range investigated; these two requirements are actually satisfied by the -PO_4^{2-} group of PA over the pH range covered by our measurements.

A further relationship is provided by Eq. 2, which can be written in the implicit form:

$$\psi'_0 - 4\pi\beta'\sigma_M - 4\pi\gamma'(\sigma_M + \Sigma_i\sigma_i) + 2\frac{RT}{F}\ln y \equiv h = 0 \quad \text{(A7)}$$

The expressions $g = 0$ and $h = 0$ of Eqs. A1 and A7 are functions of σ_M, $\{\sigma_i\}$, $\{\sigma_j\}$, and y, which are not independent variables but are functions of only two independent variables. The real roots of the two equations A1 and A7 were obtained by the Newton-Raphson iterative procedure. To ensure a rapid convergence, it was found convenient to choose as independent variables y and the average potential difference across the polar-head region:

$$\psi_1 \equiv 4\pi\gamma'(\sigma_M + \sum_i \sigma_i) = \psi'_0 - 4\pi\beta'\sigma_M + 2\frac{RT}{F}\ln y \quad \text{(A8)}$$

Moreover, it was generally necessary to mix successive approximations to y and ψ_1 before they were used as input at the next level of iteration.

When the electrolyte concentration c is varied while pH is kept constant, the surface dipole potential χ can be regarded as satisfactorily constant; hence the same is true for the quantity $\psi'_0 = (\psi_0 - \chi)$, because the applied potential E is also kept constant. However, ψ'_0 is unknown, whereas the charge density σ_M at $c = 0.1$ M is known, having been measured at each pH value. The first run of the Newton-Raphson iterative procedure at constant pH and variable c was therefore carried out for $c = 0.1$ M, using the known value of σ_M and regarding g and h as functions of y and ψ'_0. The partial derivatives of g and h with respect to y and ψ'_0 to be used in the

iterative procedure were therefore obtained from g in the form of Eq. A1 and from h in the form of Eq. A7, with σ_M constant and σ_i and σ_j expressed by Eqs. A3, A4, and A6. The ψ'_0 value obtained from the first run was then employed in the subsequent runs for the same pH and the remaining concentrations c. In these further runs, g and h were regarded as functions of ψ_1 and y, by writing them in the form

$$g = \frac{\psi'_0 - \psi_1 + 2(RT/F)\ln y}{4\pi\beta'} + \Sigma_i\sigma_i + \Sigma_j\sigma_j - A(1/y - y) = 0 \quad (9)$$

and

$$h = \frac{\beta' + \gamma'}{\beta'}\psi_1 - \frac{\gamma'}{\beta'}\left(\psi'_0 + 2\frac{RT}{F}\ln y\right) - 4\pi\gamma'\Sigma_i\sigma_i = 0 \quad (A10)$$

and differentiating them with respect to ψ_1 and y at constant ψ'_0. This procedure was repeated for all pH values.

To determine the set of parameters $\{K_i\}$, $\{K_j\}$ and γ' (or β') that provide the best fit between S_{calc} versus pH plots and S_{exp} versus pH plots, it is necessary to calculate the differential capacity C at different c and pH values. An expression for $1/C$ is obtained from Eqs. A7 and A8:

$$\frac{1}{C} = \frac{d\psi'_0}{d\sigma_M} = 4\pi\beta' + \frac{d\psi_1}{d\sigma_M} - 2\frac{RT}{Fy}\frac{dy}{d\sigma_M} \quad (A11)$$

C was determined by considering that, in differential capacity measurements, ψ'_0 varies sinusoidally about the constant value obtained at each pH by the Newton-Raphson procedure. Hence g and h must now be regarded as functions of σ_M, ψ_1, and y. If we denote the partial derivatives of the functions g and h with respect to σ_M, ψ_1, and y by the subscripts M, 1, and y, from the rules for the derivation of implicit functions we get

$$\frac{1}{C} = 4\pi\beta' + \frac{g_y h_M - h_y g_M}{g_1 h_y - h_1 g_y} - 2\frac{RT}{Fy}\frac{g_M h_1 - h_M g_1}{g_1 h_y - h_1 g_y} \quad (A12)$$

The expression of g as a function of σ_M, ψ_1, and y is provided by Eq. A1, in which σ_i and σ_j are given by Eqs. A3 and A6, and $[H^+]_\beta$ takes the form

$$[H^+]_\beta = c_{H^+}y^2\exp\left[-\frac{F}{RT}\frac{\gamma'}{\beta' + \gamma'}(4\pi\beta'\sigma_M + \psi_1)\right] \quad (A13)$$

Analogously, the expression of h as a function of σ_M, ψ_1, and y is

$$h = \psi_1 - 4\pi\gamma'(\sigma_M + \Sigma_i\sigma_i) \quad (A14)$$

where σ_i is given by Eqs. A3 and A13.

Thanks are due to ENEA, Italy, for a Ph.D. fellowship to FTB, during the tenure of which the present results were obtained. The financial support of the Ministero dell'Università e della Ricerca Scientifica e Tecnologica and of the Consiglio Nazionale delle Ricerche is gratefully acknowledged.

REFERENCES

Antonenko, Y. N., O. N. Kovbasnjuk, and L. S. Yaguzhinsky. 1993. Evidence in favor of the existence of a kinetic barrier for proton transfer from a surface of bilayer phospholipid membrane to bulk water. *Biochim. Biophys. Acta.* 1150:45–50.

Becucci, L., M. R. Moncelli, and R. Guidelli. 1996. Surface charge density measurements on mercury electrodes covered by phospholipid monolayers. *J. Electroanal. Chem.* 413:187–193.

Bockris, J. O'M., M. A. V. Devanathan, and K. Muller. 1965. On the structure of charged interfaces. *In* Proceedings of the First Australian Conference on Electrochemistry. J. A. Friend and F. Gutmann, editors. Pergamon Press, Elmsford, NY. 832–863.

Damaskin, B. B., and A. N. Frumkin. 1974. Potential of zero charge, interaction of metals with water and adsorption of organic substances. III. The role of the water dipoles in the structure of the dense part of the electric double layer. *Electrochim. Acta.* 19:173–176.

Flewelling, R. F., and W. L. Hubbell. 1986. The membrane dipole potential in a total membrane potential model. Applications to hydrophobic ion interactions with membranes. *Biophys. J.* 49:541–552.

Gawrisch, K., R. Delaney, J. Zimmerberg, V. A. Parsegian, R. P. Rand, and N. Fuller. 1992. Membrane dipole potentials, hydration forces, and the ordering of water at membrane surfaces. *Biophys. J.* 61:1213–1223.

Gutman, M., and E. Nachliel 1990. The dynamic aspects of proton transfer processes. *Biochim. Biophys. Acta.* 1015:391–414.

Heberle, J., J. Riesle, G. Thiedemann, D. Oesterhelt, and N. A. Dencher. 1994. Proton migration along the membrane surface and retarded surface to bulk transfer. *Nature.* 370:379–382.

Honig, B. H., W. L. Hubbell, and R. F. Flewelling. 1986. Electrostatic interactions in membranes and proteins. *Annu. Rev. Biophys. Biophys. Chem.* 15:163–193.

Kasianowicz, J., R. Benz, M. Gutman, and S. Mc Laughlin. 1987. Reply to: Lateral diffusion of protons along phospholipid monolayers. *J. Membr. Biol.* 99:227.

Kell, D. B. 1979. On the functional proton current pathway of electron transport phosphorylation. An electrodic view. *Biochim. Biophys. Acta.* 549:55–99.

Levine, S., G. M. Bell, and D. Calvert. 1962. The discreteness of charge effect in electric double-layer theory. *Can. J. Chem.* 40:518–537.

Levine, S., J. Mingings, and G. M. Bell. 1965. The diffuse layer correction to the discrete-ion effect in electric double-layer theory. *Can. J. Chem.* 43:2834–2865.

Levine, S., K. Robinson, G. M. Bell, and J. Mingins. 1972. The discreteness-of-charge effect at charged aqueous interfaces. I. General theory for single adsorbed ion species. *J. Electraoanal. Chem.* 38:253–269.

MacDonald, R. C., S. A. Simon, and E. Baer. 1976. Ionic influences of the phase transition of dipalmitoylphosphatidylserine. *Biochemistry.* 15: 885–891.

Matinyan, N. S., I. A. Ershler, and I. G. Abidor. 1985. Proton equilibrium on the surfaces of bilayer lipid membranes. *Biol. Membr.* 1:451–477.

McLaughlin, S. 1977. Electrostatic potentials at membrane-solution interfaces. *Curr. Top. Membr. Transp.* 9:71–137.

Miller, I. R. 1981. Structural and energetics aspects of charge transport in lipid layers and biological membranes. *In* Topics in Bioelectrochemistry and Bioenergetics. G. Milazzo, editor. Wiley, Chichester. 194–225.

Moncelli, M. R., and L. Becucci. 1995. The intrinsic pK_a values for phosphatidic acid in monolayers deposited on mercury electrodes. *J. Electroanal. Chem.* 385:183–189.

Moncelli, M. R., L. Becucci, and R. Guidelli. 1994. The intrinsic pK_a values for phosphatidylcholine, phosphatidylethanolamine and phosphatidylserine in monolayers deposited on mercury electrodes. *Biophys. J.* 66:1969–1980.

Moncelli, M. R., L. Becucci, R. Herrero, and R. Guidelli. 1995. Adsorption of tetraphenylphosphonium and tetraphenylborate in self-assembled phosphatidylcholine and phosphatidylserine monolayers deposited on mercury electrodes. *J. Phys. Chem.* 99:9940–9951.

Morgan, H., D. M. Taylor, and O. N. Oliveira Jr.. 1988. Two-dimensional proton conduction at a membrane surface: influence of molecular packing and hydrogen bonding. *Chem. Phys. Lett.* 150:311–314.

Nachliel E., and M. Gutman. 1988. Time-resolved proton-phospholipid interaction. Methodology and kinetic analysis. *J. Am. Chem. Soc.* 110: 2629–2635.

Nelson, A., and A. Benton. 1986. Phospholipid monolayers at the mercury/water interface. *J. Electroanal. Chem.* 202:253–270.

Ohki, S., and R. Kurland. 1981. Surface potential of phosphatidylserine monolayers. II. Divalent and monovalent ion binding. *Biochim. Biophys. Acta.* 645:170–176.

Polle, A., and W. Junge. 1989. Proton diffusion along the membrane surface of thylacoids is not enhanced over that in bulk water. *Biophys. J.* 56:27–31.

Prats, M., J. Teissié, and J.-F. Tocanne. 1986. Lateral proton conduction at lipid-water interfaces and its implications for the chemiosmotic-coupling hypothesis. *Nature.* 322:756–758.

Prats, M., J-F. Tocanne, and J. Teissié. 1985. Lateral proton conduction at a lipid/water interface. Its modulation by physical parameters. Experimental and mathematical approaches. *Eur. J. Biochem.* 149:663–668.

Teissié, J., M. Prats, P. Soucaille, and J.-F. Tocanne. 1985. Evidence for conduction of protons along the interface between water and a polar lipid monolayer. *Proc. Natl. Acad. Sci. USA.* 82:3217–3221.

Trasatti, S. 1975. Water dipole contribution to the potential drop across the double layer. The charge of zero net dipole orientation. *J. Electroanal. Chem.* 64:128–134.

Tsui, F. C., D. M. Ojcius, and W. L. Hubbel. 1986. The intrinsic pK_a values for phosphatidylserine and phosphatidylethanolamine in phosphatidylcholine host bilayers. *Biophys. J.* 49:459–468.

Zheng, C., and G. Vanderkooi. 1992. Molecular origin of the internal dipole potential in lipid bilayers: calculation of the electrostatic potential. *Biophys. J.* 63:935–941.